Electronic Supplementary Material (ESI) for New Journal of Chemistry.
This journal is © The Royal Society of Chemistry and the Centre National de la Recherche Scientifique 2021

**Synthesis and coordination of a hybrid phosphinoferrocene sulfonamide ligand**

Věra Varmužová, Filip Horký and Petr Štěpnička*

# SUPPORTING INFORMATION

**Contents**

**Additional structural diagrams**

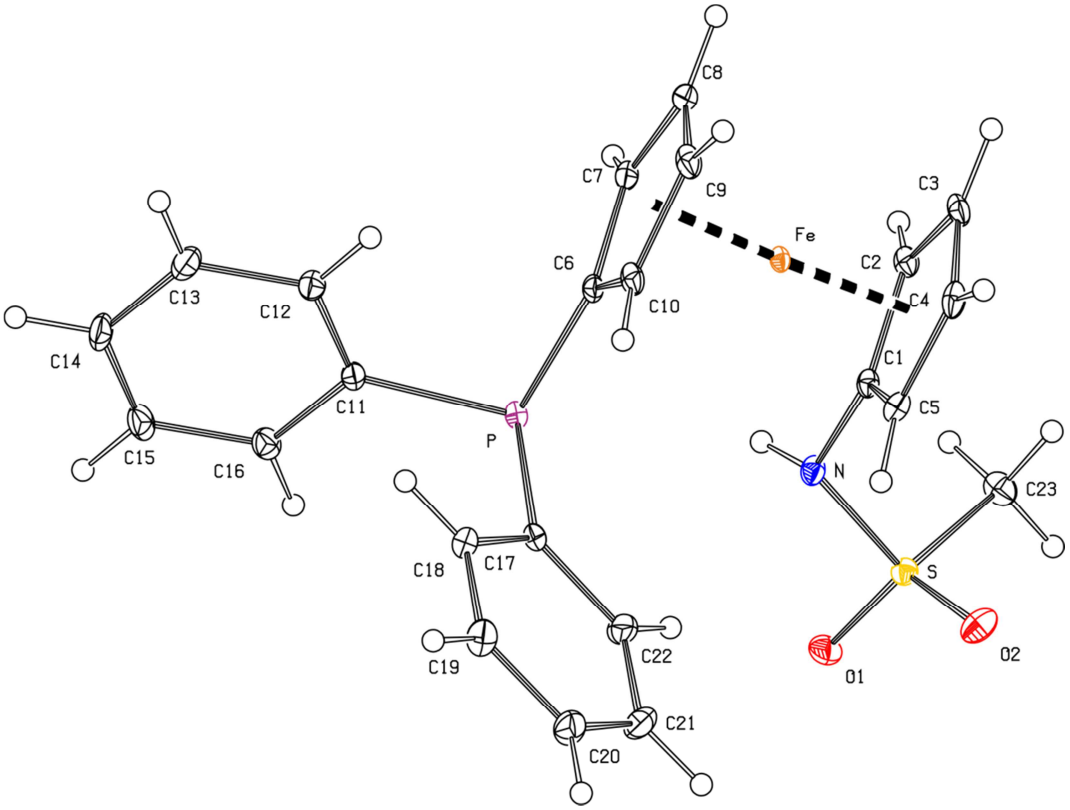


**Figure S1.** PLATON plot of the molecular structure of **1** showing displacement ellipsoids at the 30% probability level.

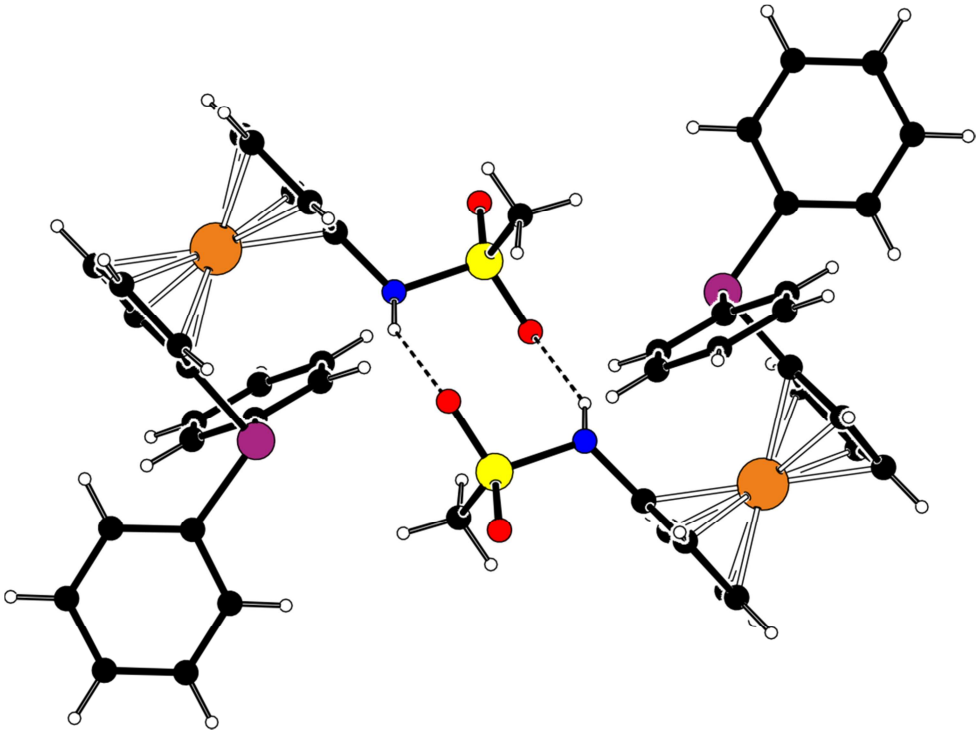

**Figure S2.** View of the hydrogen-bonded dimeric motif in the structure of **1**.

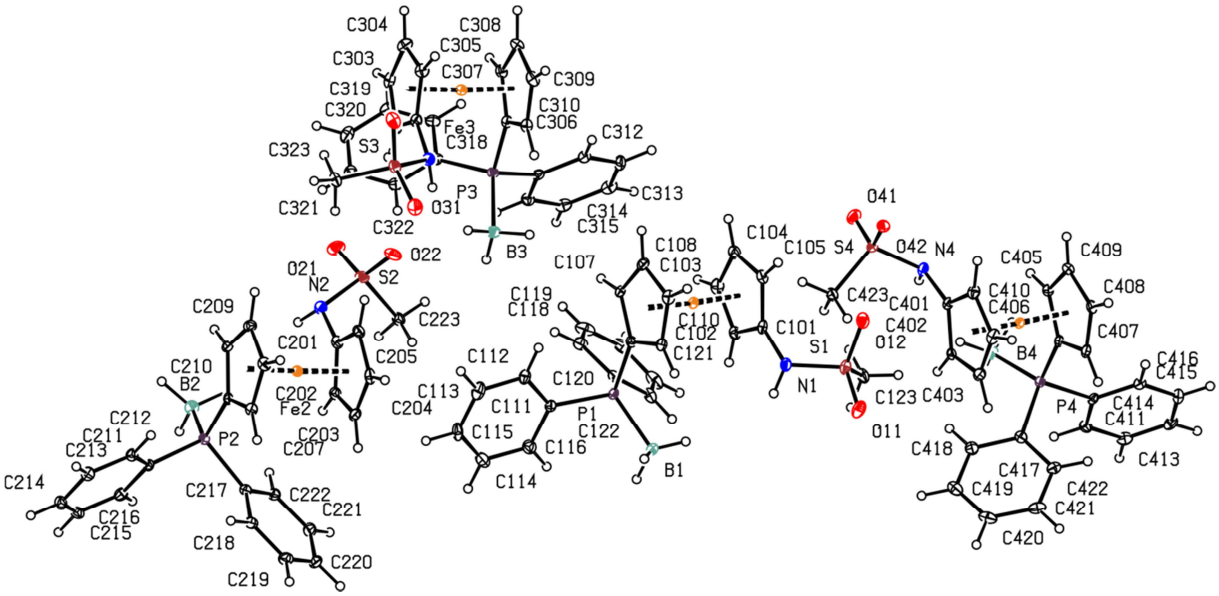


**Figure S3.** PLATON plot of the four independent molecules in the crystal structure of **2** at the 30% probability level.

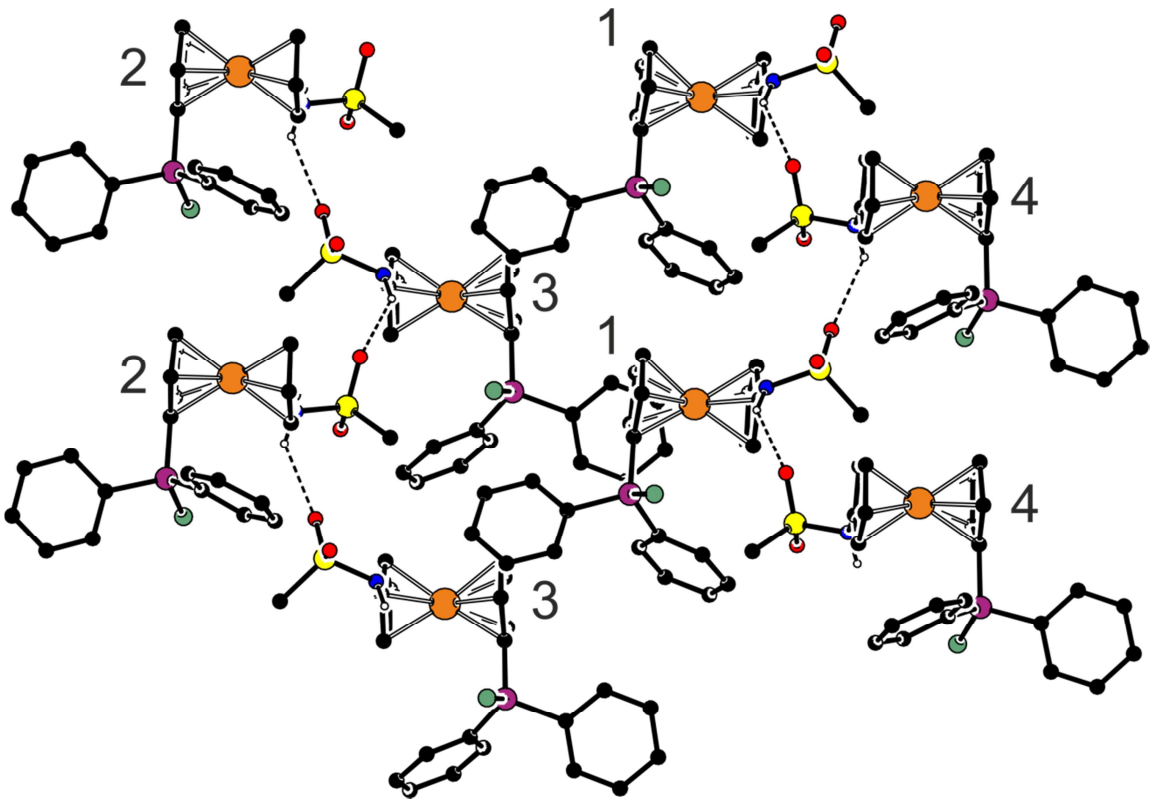


**Figure S4.** Section of the hydrogen-bonded chains in the structure of **2** (only the NH hydrogens are shown for clarity and hydrogen bonds are indicated by dashed lines). The independent molecules are distinguished by numbers.

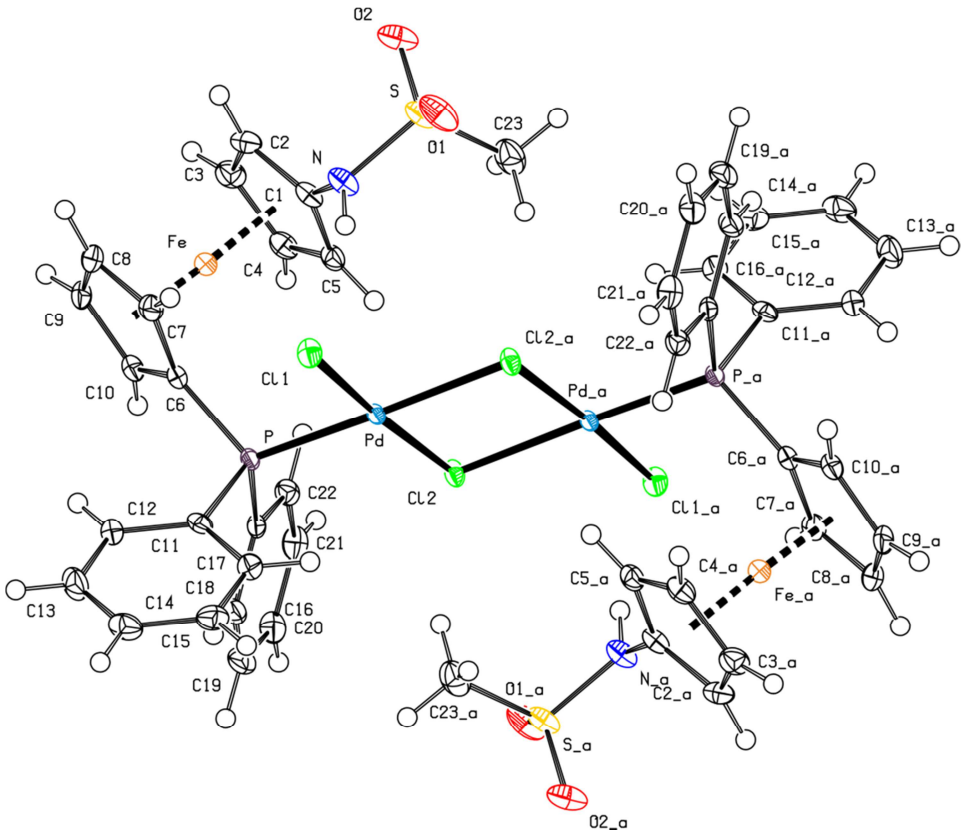


**Figure S5.** PLATON plot of the complex molecule in the structure of **4**·2$CHCl_3$ with 30% probability ellipsoids (Note: the half of the molecule is generated by crystallographic inversion).

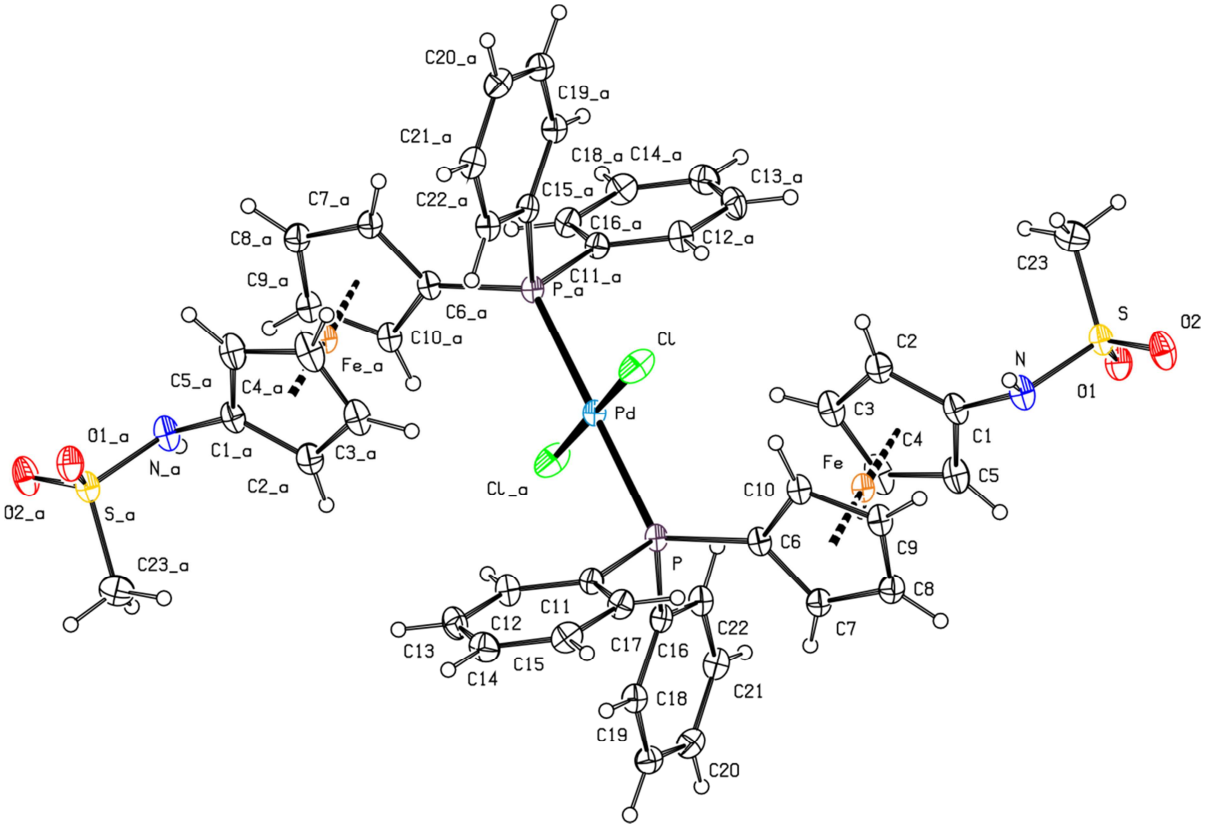


**Figure S6.** PLATON plot of the molecular structure of **5** showing 30% probability ellipsoids (Note: the half of the molecule is generated by crystallographic inversion).

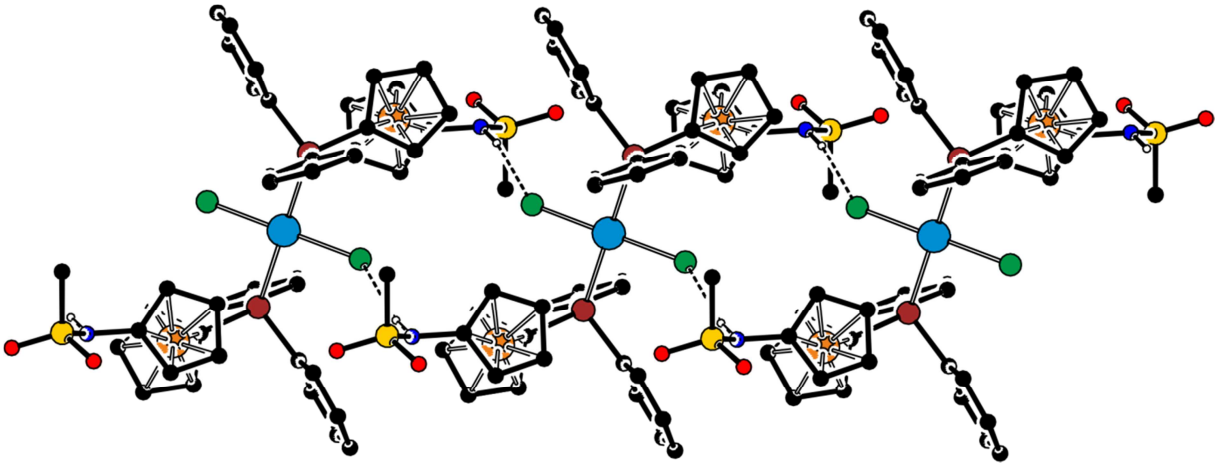

**Figure S7.** Section of the infinite, hydrogen-bonded chain in the structure of **5**.

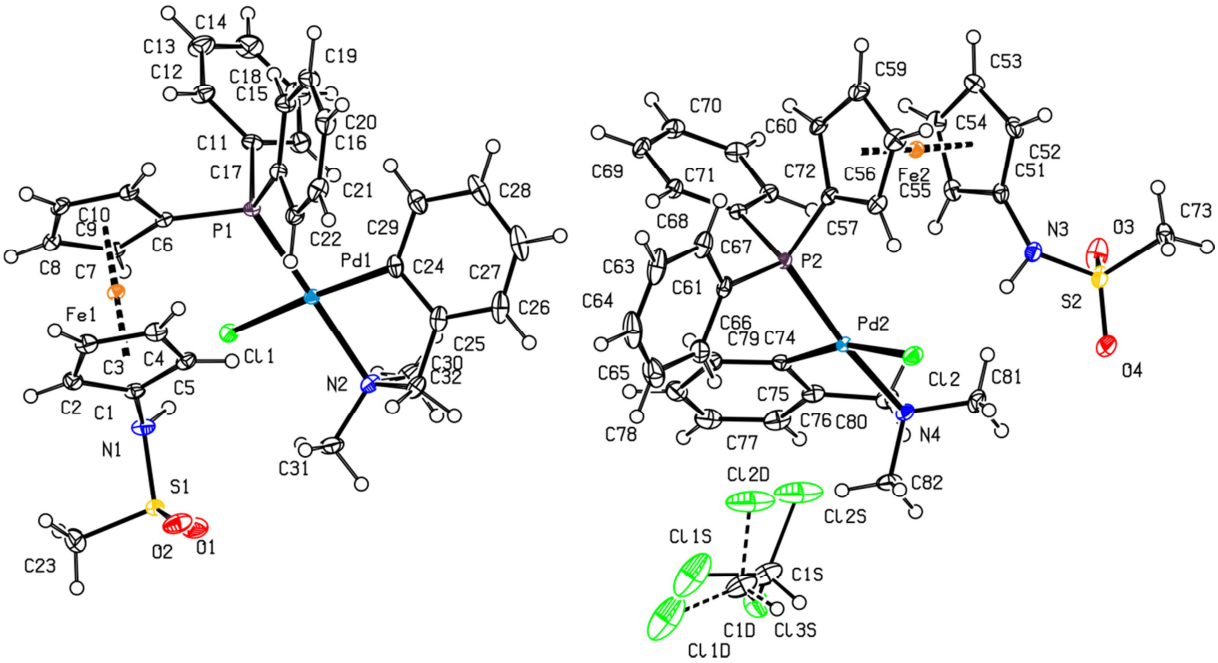


**Figure S8.** PLATON plot of the molecular structure of **6**·½$CHCl_3$ (30% probability ellipsoids).

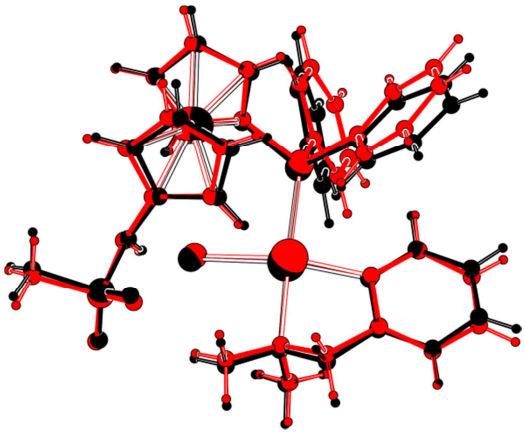

**Figure S9.** Least-squares overlap of the independent molecules in the structure of **6**·½$CHCl_3$.

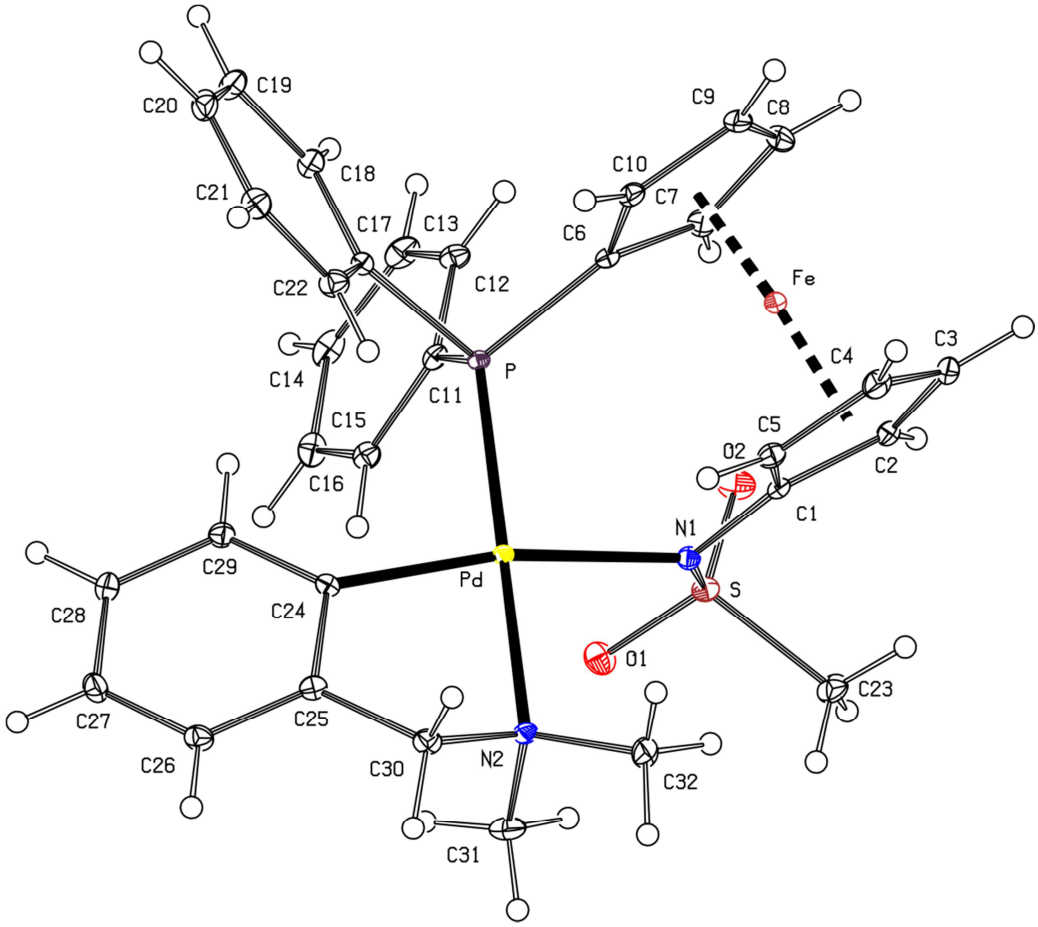


**Figure S10.** PLATON plot of the molecular structure of **7** (displacement ellipsoids enclose the 30% probability level).

**Table S1** Selected crystallographic data and structure refinement parameters[a]

| Compound | **1** | **2** | **4**·2$CHCl_3$ |
|---|---|---|---|
| Formula | $C_{23}H_{22}FeNO_2PS$ | $C_{23}H_{25}BFeNO_2PS$ | $C_{48}H_{46}Cl_{10}Fe_2N_2O_4P_2Pd_2S_2$ |
| *M* | 463.29 | 477.13 | 1519.93 |
| Crystal system | triclinic | orthorhombic | triclinic |
| Space group | *P*–1 (no. 2) | $Pca2_1$ (no. 29)[d] | *P*–1 (no. 2) |
| *T* (K) | 120(2) | 120(2) | 120(2) |
| *a* [Å] | 8.8310(5) | 18.5588(9) | 10.8367(6) |
| *b* [Å] | 9.6737(5) | 9.0762(4) | 11.5827(7) |
| *c* [Å] | 12.2527(6) | 51.788(3) | 11.5985(7) |
| α [°] | 99.502(2) | 90 | 84.816(2) |
| β [°] | 95.461(2) | 90 | 75.910(2) |
| γ [°] | 91.567(2) | 90 | 79.007(2) |
| *V* [Å]$^3$ | 1026.69(9) | 8723.3(7) | 1384.6(1) |
| *Z* | 2 | 16 | 1 |
| μ(Mo Kα) [$mm^{-1}$] | 0.934 | 7.292 | 1.814 |
| Diffrns collected | 20233 | 67871 | 27631 |
| Independent diffrns | 4736 | 16364 | 6372 |
| Observed[a] diffrns | 4343 | 15405 | 5698 |
| $R_{int}$[b] [%] | 2.20 | 3.68 | 2.41 |
| No. of parameters | 264 | 1085 | 326 |
| *R*[c] obsd diffrns [%] | 2.49 | 3.19 | 2.49 |
| *R*, *wR*[c] all data [%] | 2.89, 6.34 | 3.45, 7.98 | 3.03, 5.73 |
| Δρ [e $Å^{-3}$] | 0.61, −0.50 | 0.45, −0.43 | 0.80, −0.64 |

[a] Diffractions with $I > 2\sigma(I)$. [b] Definitions: $R_{int} = \Sigma\left|F_o^2 - F_o^2(\text{mean})\right|/\Sigma F_o^2$, where $F_o^2$(mean) denoted the average intensity of symmetry-equivalent diffractions. [c] $R = \Sigma\left|\left|F_o\right| - \left|F_c\right|\right|/\Sigma\left|F_o\right|$, $wR = [\Sigma\{w(F_o^2 - F_c^2)^2\}/\Sigma w(F_o^2)^2]^{1/2}$. [d] Flack's enantiomorph parameter: 0.008(2).

**Table S1 continued**

| Compound | **5** | **6**·½$CHCl_3$ | **7** |
|---|---|---|---|
| Formula | $C_{46}H_{44}Cl_2Fe_2N_2O_4P_2PdS_2$ | $C_{32.5}H_{34.5}Cl_{2.5}FeN_2O_2PPdS$ | $C_{32}H_{33}FeN_2O_2PPdS$ |
| *M* | 1103.89 | 799.02 | 702.88 |
| Crystal system | *P*–1 (no. 2) | *P*–1 (no. 2) | $P2_1/n$ (no. 14) |
| Space group | triclinic | triclinic | monoclinic |
| *T* (K) | 120(2) | 120(2) | 120(2) |
| *a* [Å] | 8.8684(8) | 10.6520(5) | 13.4617(5) |
| *b* [Å] | 11.294(1) | 16.9584(8) | 13.7207(5) |
| *c* [Å] | 12.122(1) | 20.2403(9) | 15.3668(7) |
| α [°] | 101.103(2) | 109.208(1) | 90 |
| β [°] | 93.464(2) | 101.163(2) | 94.062(1) |
| γ [°] | 105.757(2) | 100.816(2) | 90 |
| *V* [Å]$^3$ | 1138.4(2) | 3260.3(3) | 2831.2(2) |
| *Z* | 1 | 4 | 4 |
| μ(Mo Kα) [mm$^{-1}$] | 11.166 | 1.348 | 1.312 |
| Diffrns collected | 22389 | 63690 | 43435 |
| Independent diffrns | 4447 | 14991 | 6491 |
| Observed[a] diffrns | 4157 | 13669 | 5955 |
| $R_{int}$[b] [%] | 4.99 | 2.06 | 2.64 |
| No. of parameters | 278 | 791 | 365 |
| *R*[c] obsd diffrns [%] | 3.84 | 2.67 | 1.99 |
| *R*, *wR*[c] all data [%] | 4.08, 10.4 | 3.09, 6.37 | 2.31, 5.12 |
| Δρ [e Å$^{-3}$] | 1.56, –0.90 | 1.24, –1.47 | 0.56, –0.56 |

**Copies of the NMR spectra**

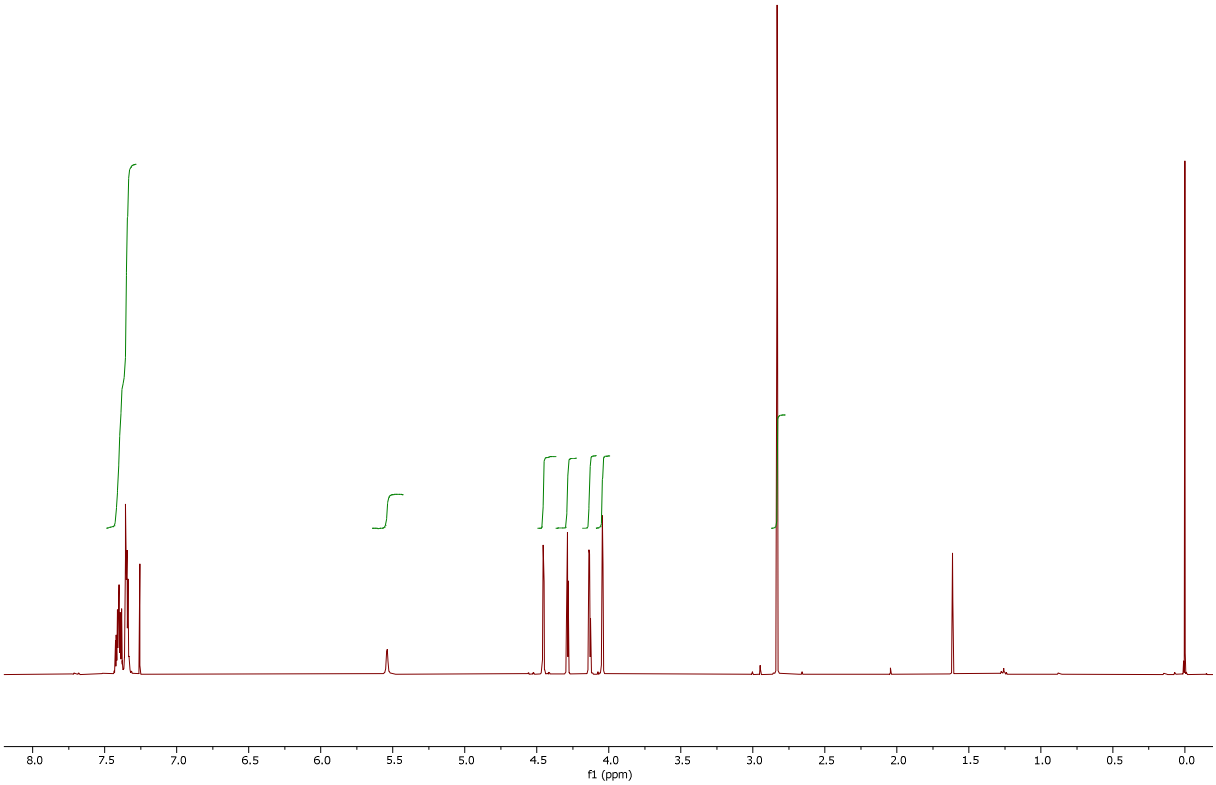


**Figure S11.** $^{1}H$ NMR (400 MHz, $CDCl_3$) spectrum of **1**.

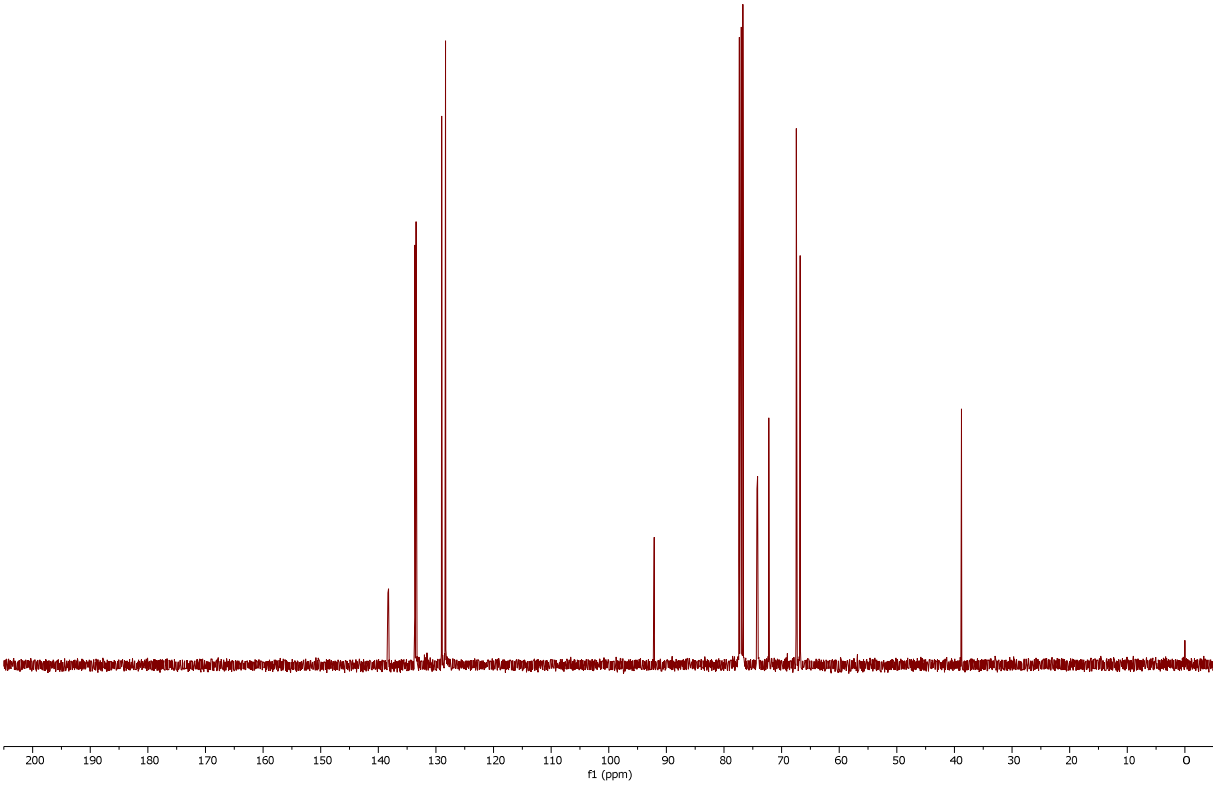


**Figure S12.** $^{13}C\{^{1}H\}$ NMR (101 MHz, $CDCl_3$) spectrum of **1**.

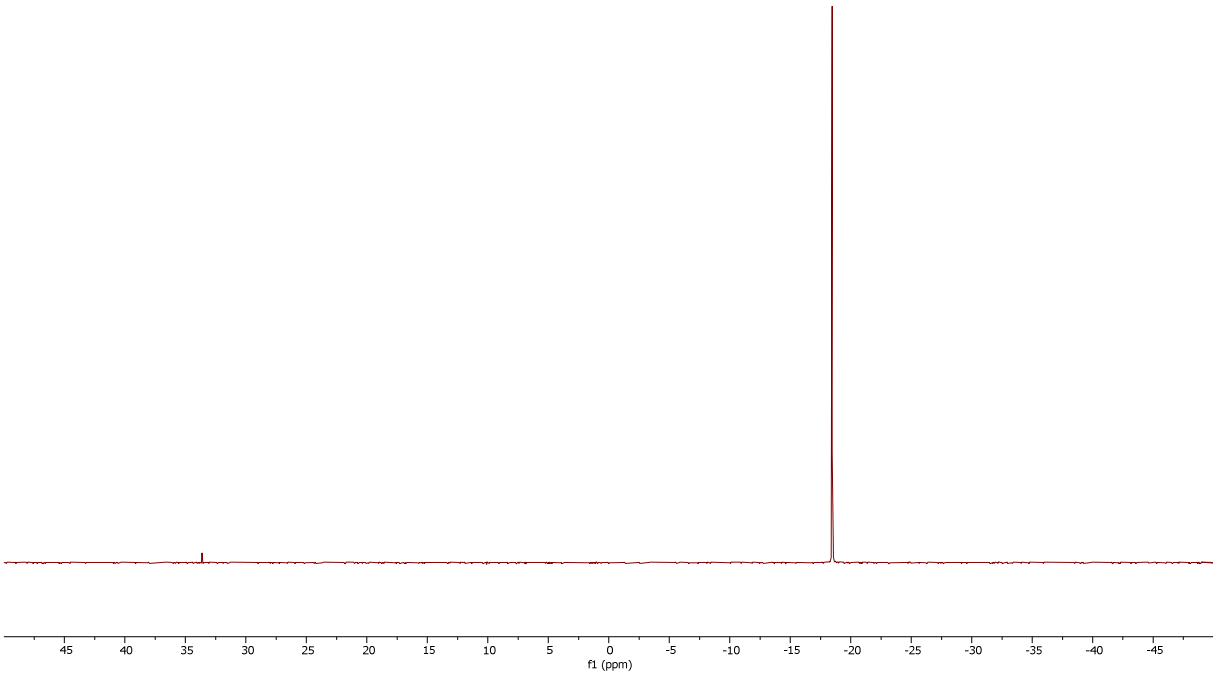


**Figure S13.** $^{31}P\{^{1}H\}$ NMR (162 MHz, $CDCl_3$) spectrum of **1**.

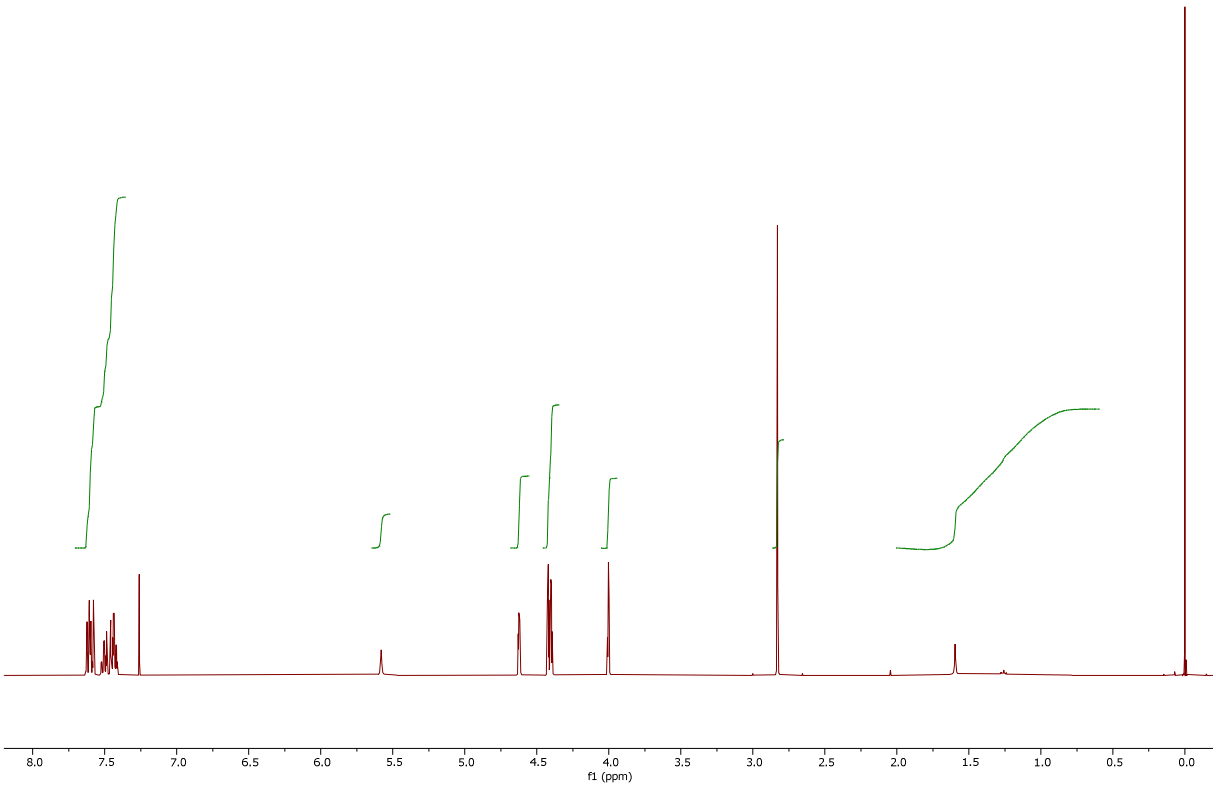


**Figure S14.** $^{1}H$ NMR (400 MHz, $CDCl_3$) spectrum of **2**.

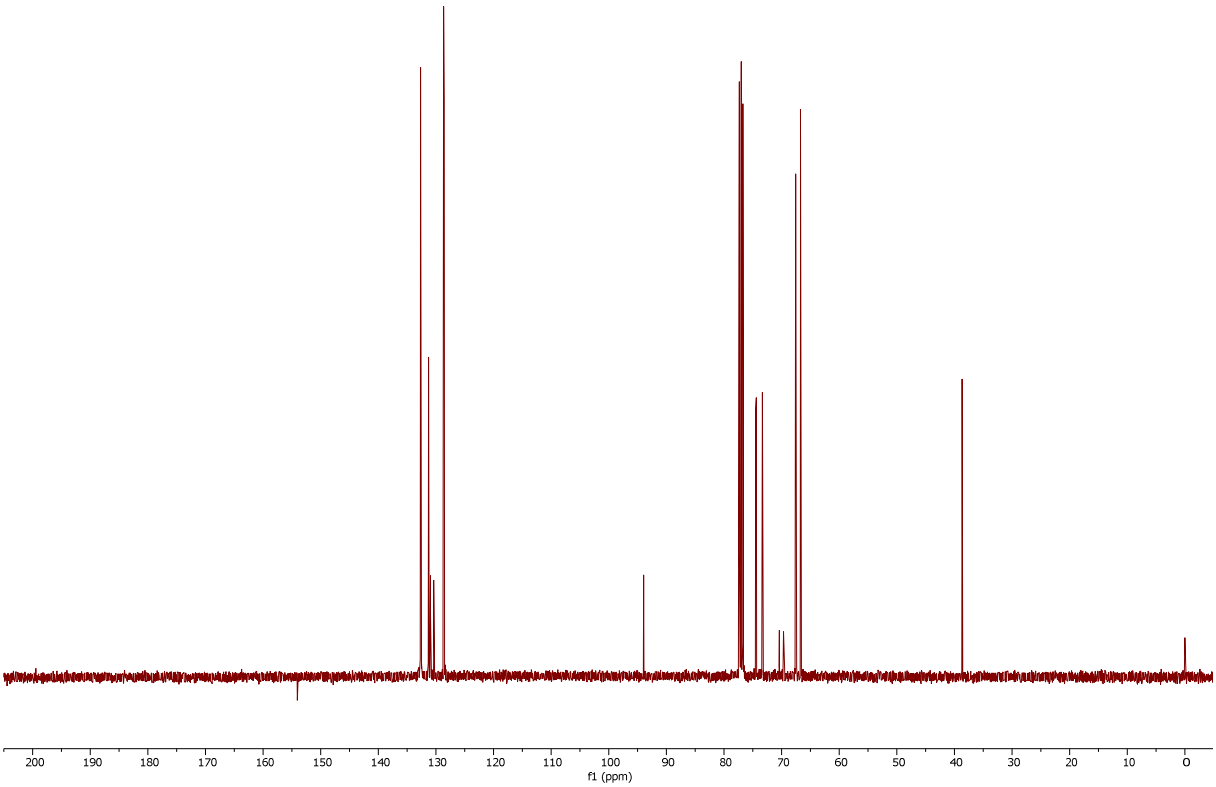


**Figure S15.** $^{13}C\{^{1}H\}$ NMR (101 MHz, $CDCl_3$) spectrum of **2**.

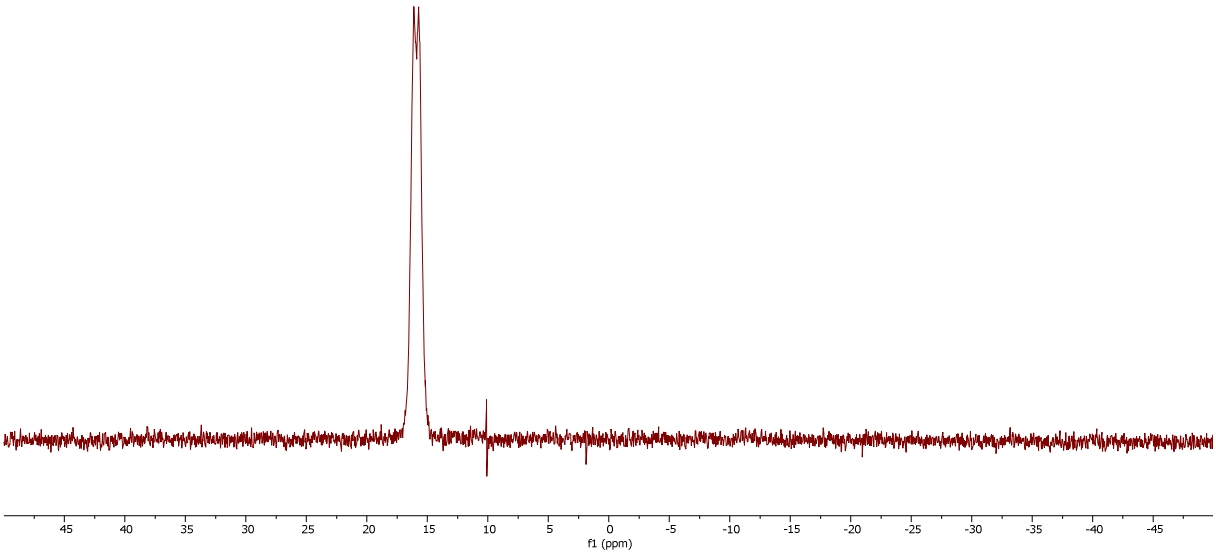


**Figure S16.** $^{31}P\{^{1}H\}$ NMR (162 MHz, $CDCl_3$) spectrum of **2**.

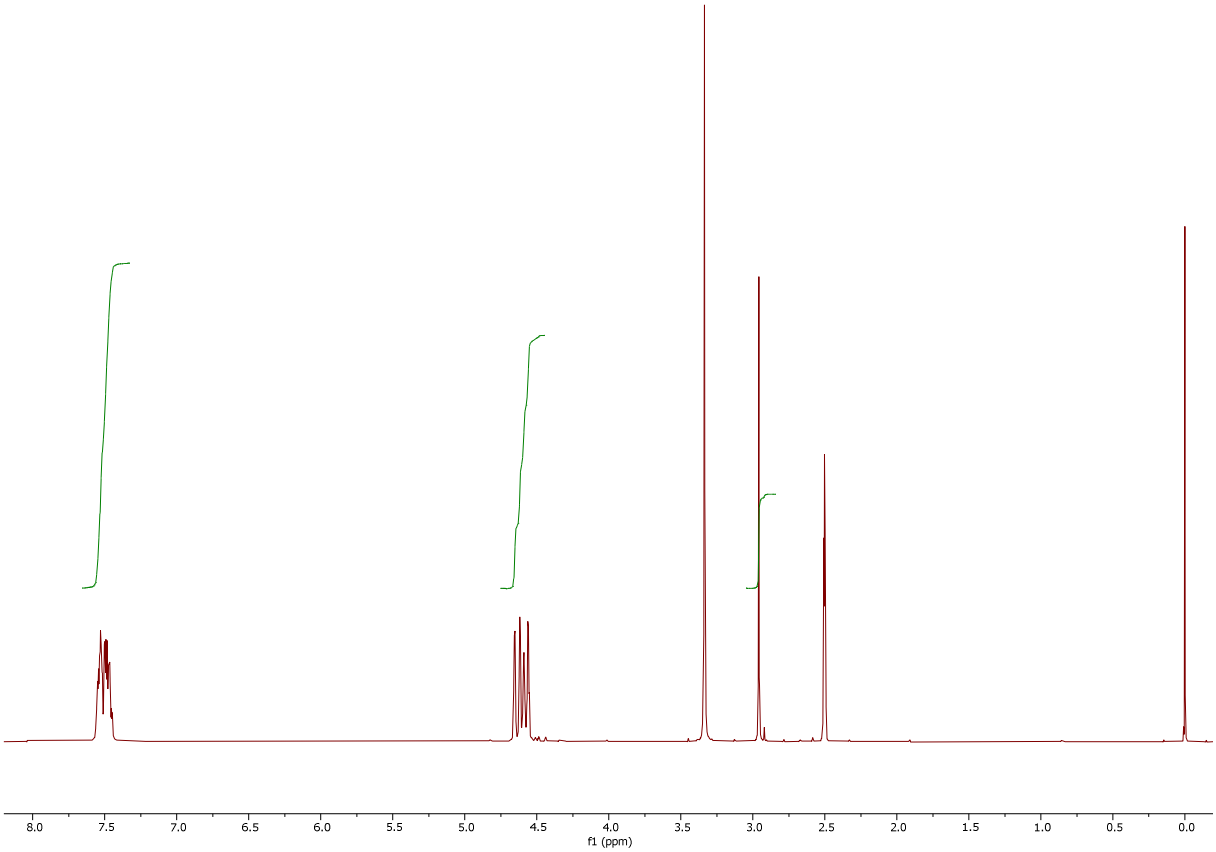


**Figure S17.** $^{1}H$ NMR (400 MHz, dmso-$d_6$) spectrum of **4**.

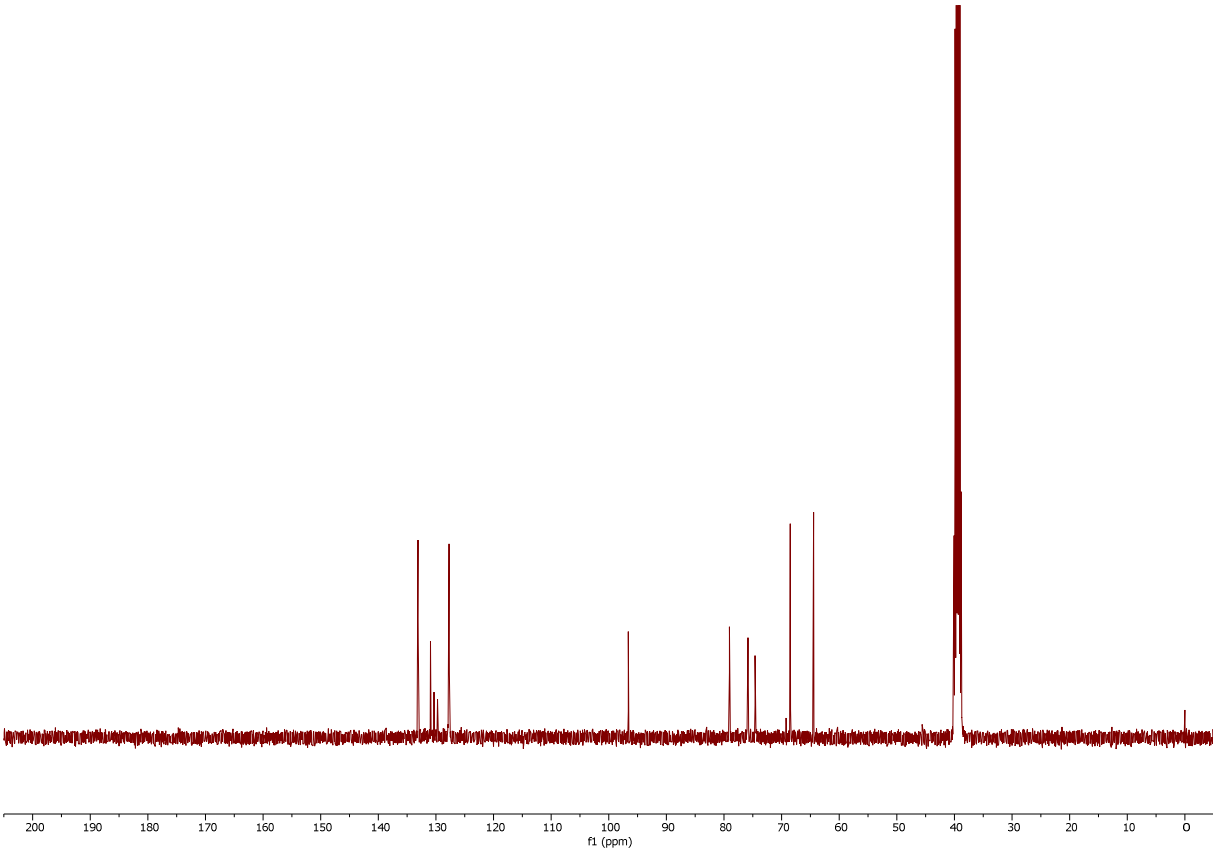


**Figure S18.** $^{13}C\{^{1}H\}$ NMR (101 MHz, dmso-$d_6$) spectrum of **4**.

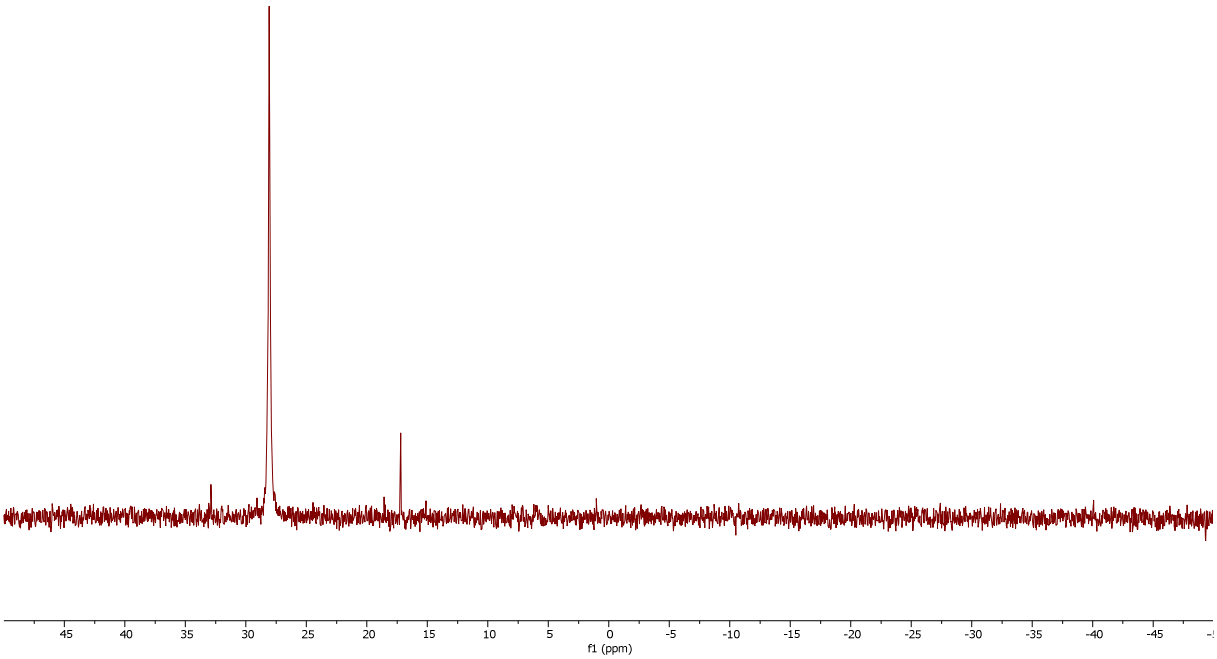


**Figure S19.** $^{31}P\{^{1}H\}$ NMR (162 MHz, dmso-$d_6$) spectrum of **4**.

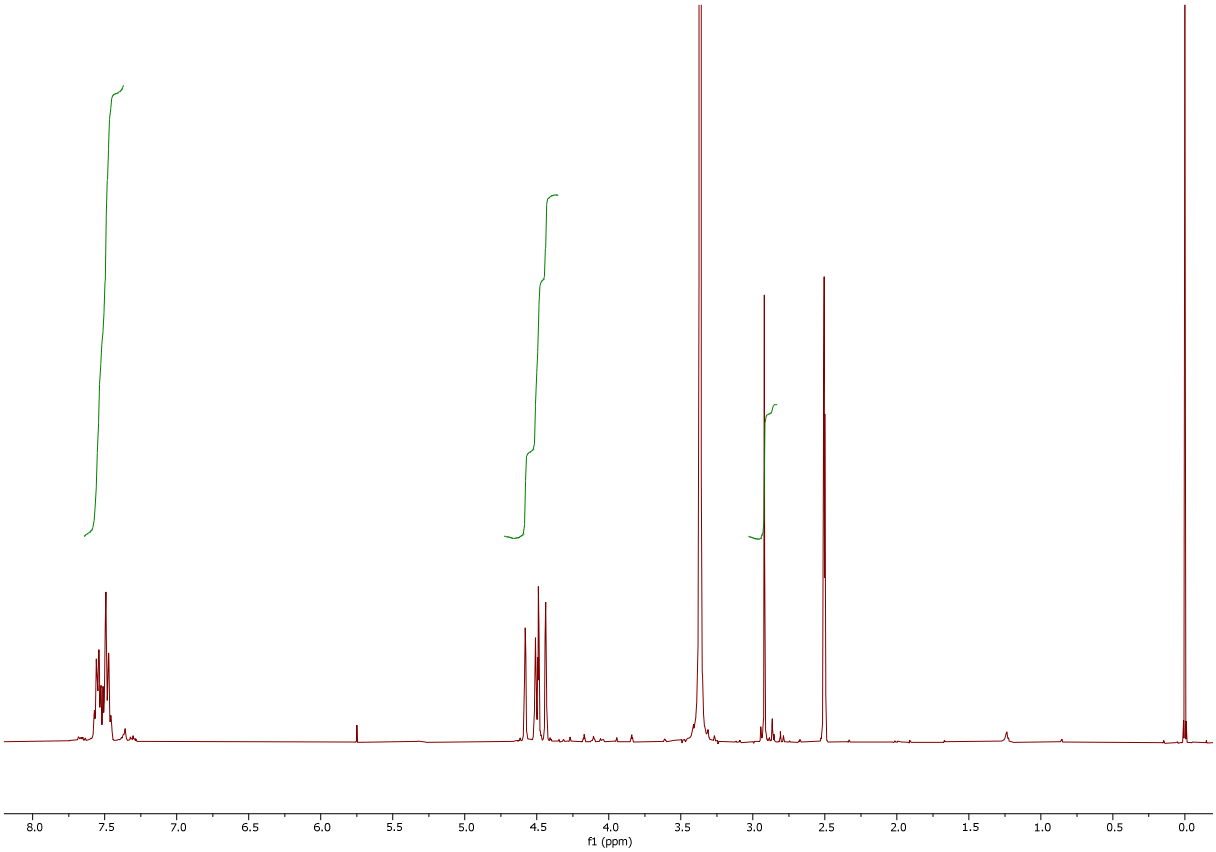


**Figure S20.** $^{1}H$ NMR (400 MHz, dmso-$d_6$) spectrum of **5**.

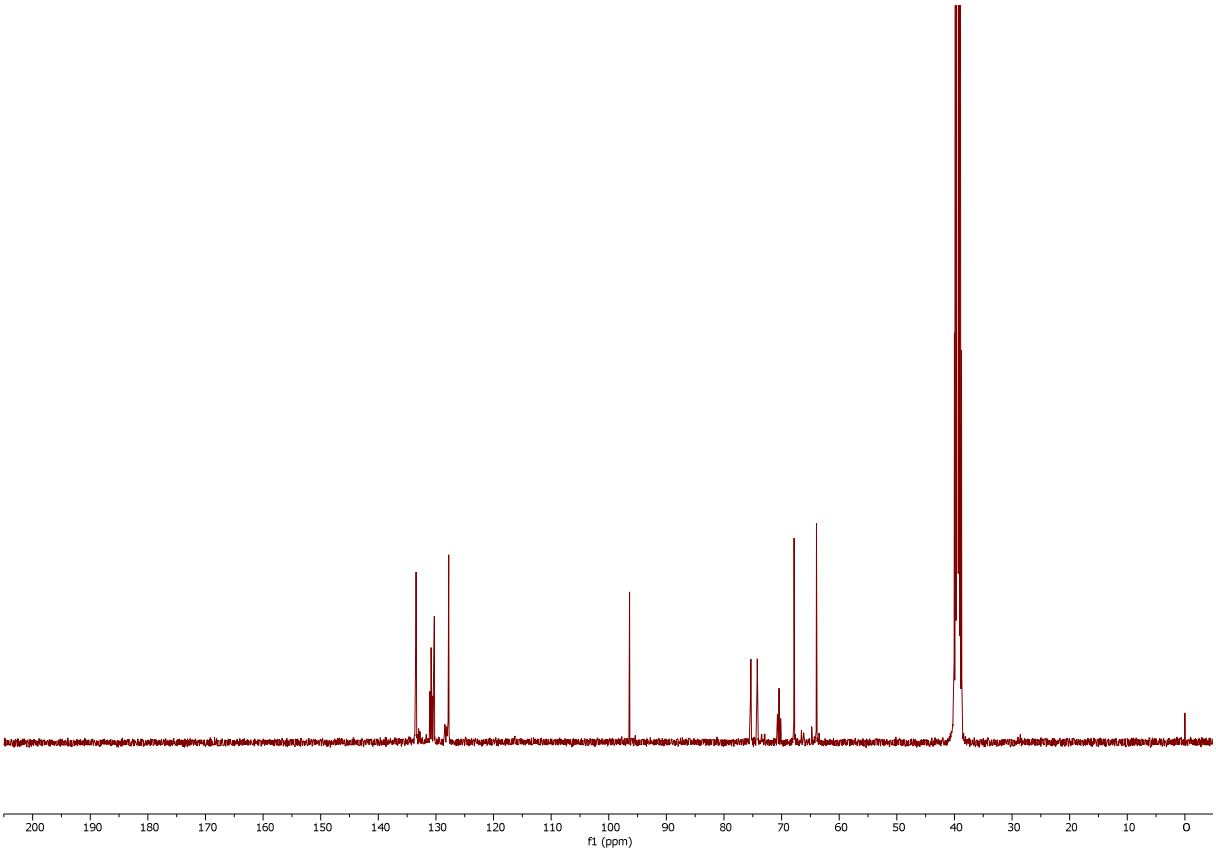


**Figure S21.** $^{13}C\{^{1}H\}$ NMR (101 MHz, dmso-$d_6$) spectrum of **5**.

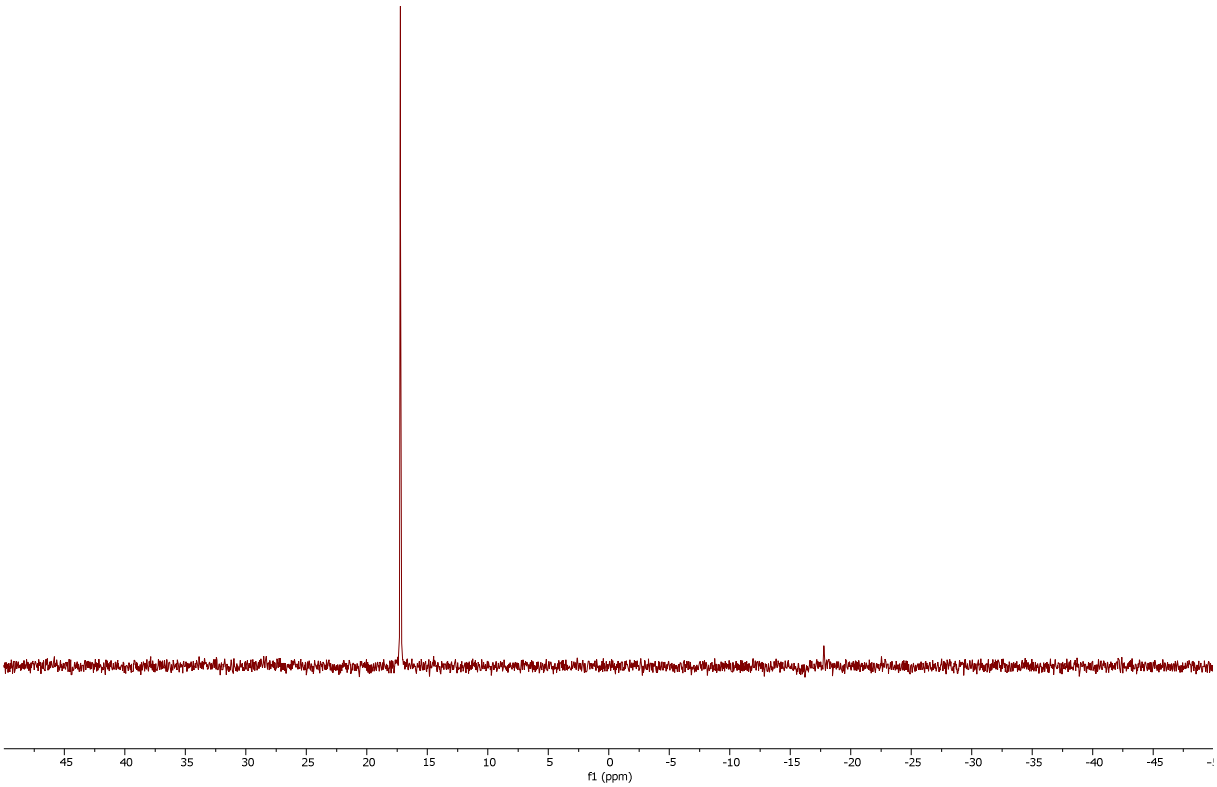


**Figure S22.** $^{31}P\{^{1}H\}$ NMR (162 MHz, dmso-$d_6$) spectrum of **5**.

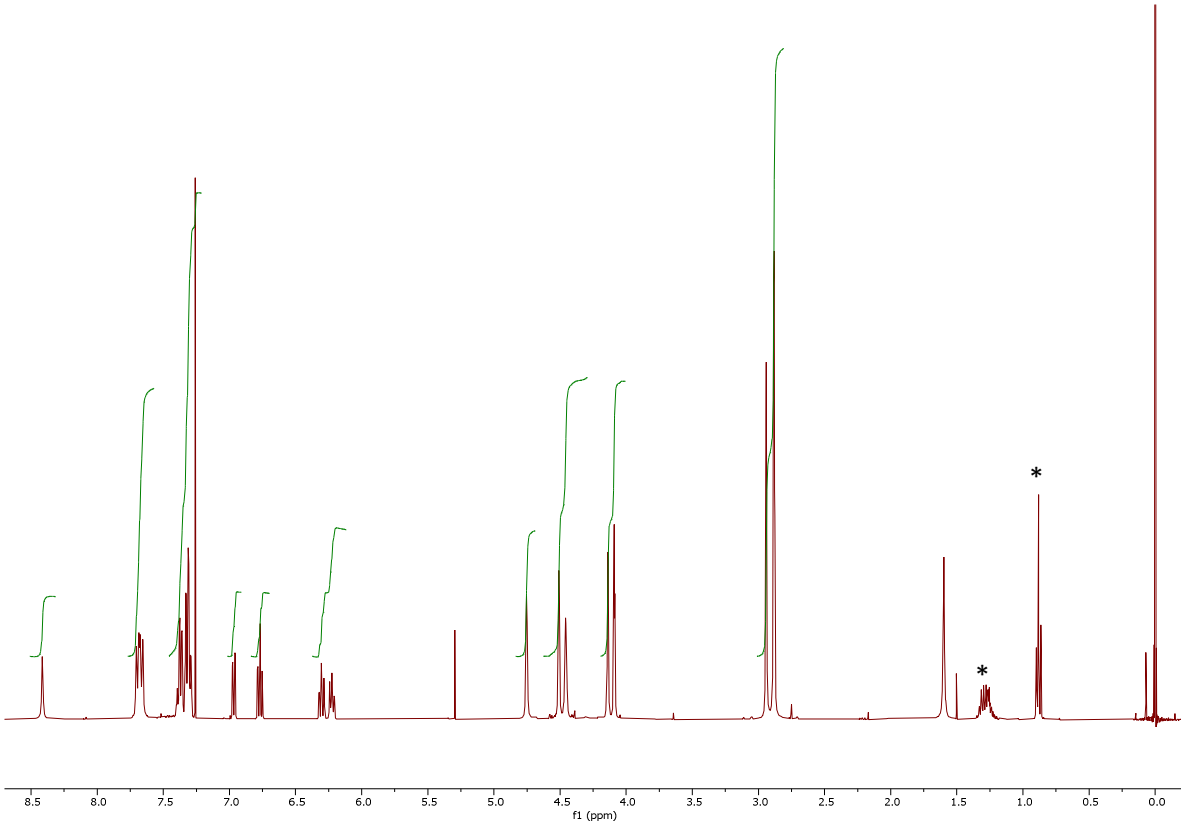


**Figure S23.** $^{1}H$ NMR (400 MHz, $CDCl_3$) spectrum of **6** (signals marked with * are due to residual pentane used to precipitate the product).

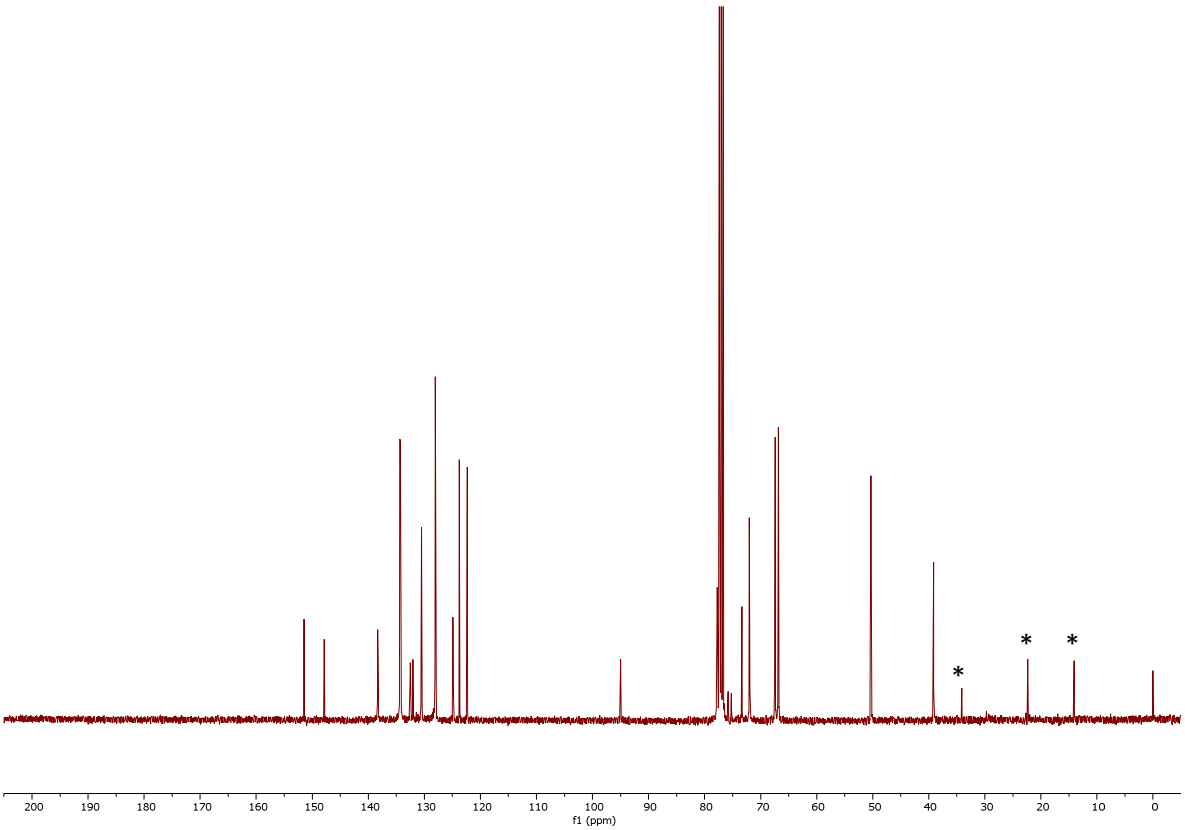


**Figure S24.** $^{13}C\{^{1}H\}$ NMR (101 MHz, $CDCl_3$) spectrum of **6** (signals marked with * are due to residual pentane used to precipitate the product).

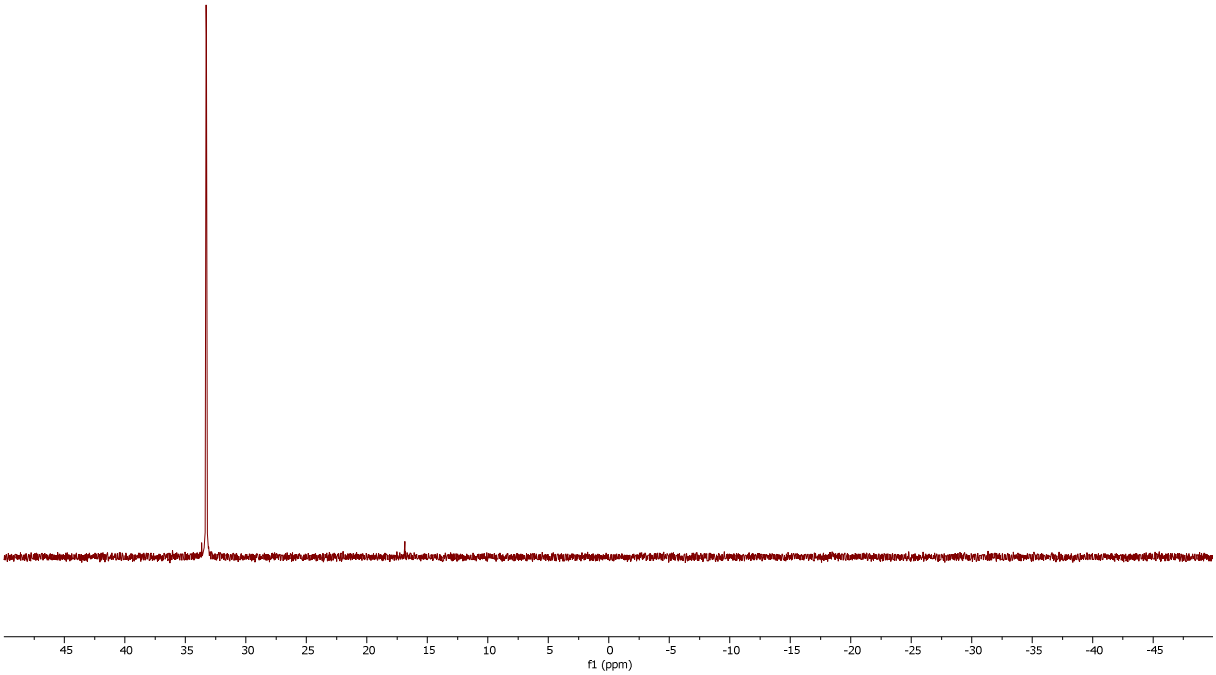


**Figure S25.** $^{31}P\{^{1}H\}$ NMR (162 MHz, $CDCl_3$) spectrum of **6**.

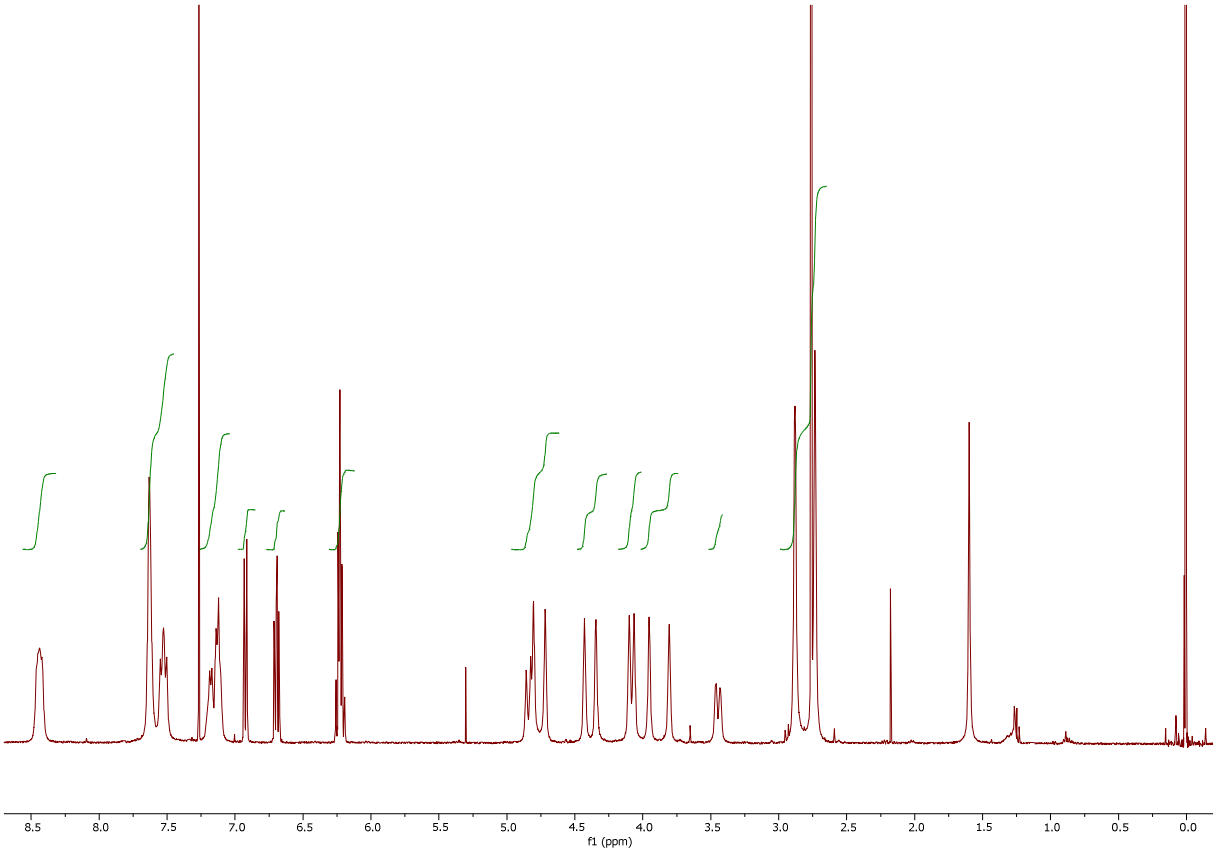


**Figure S26.** $^{1}H$ NMR (400 MHz, $CDCl_3$) spectrum of **7**.

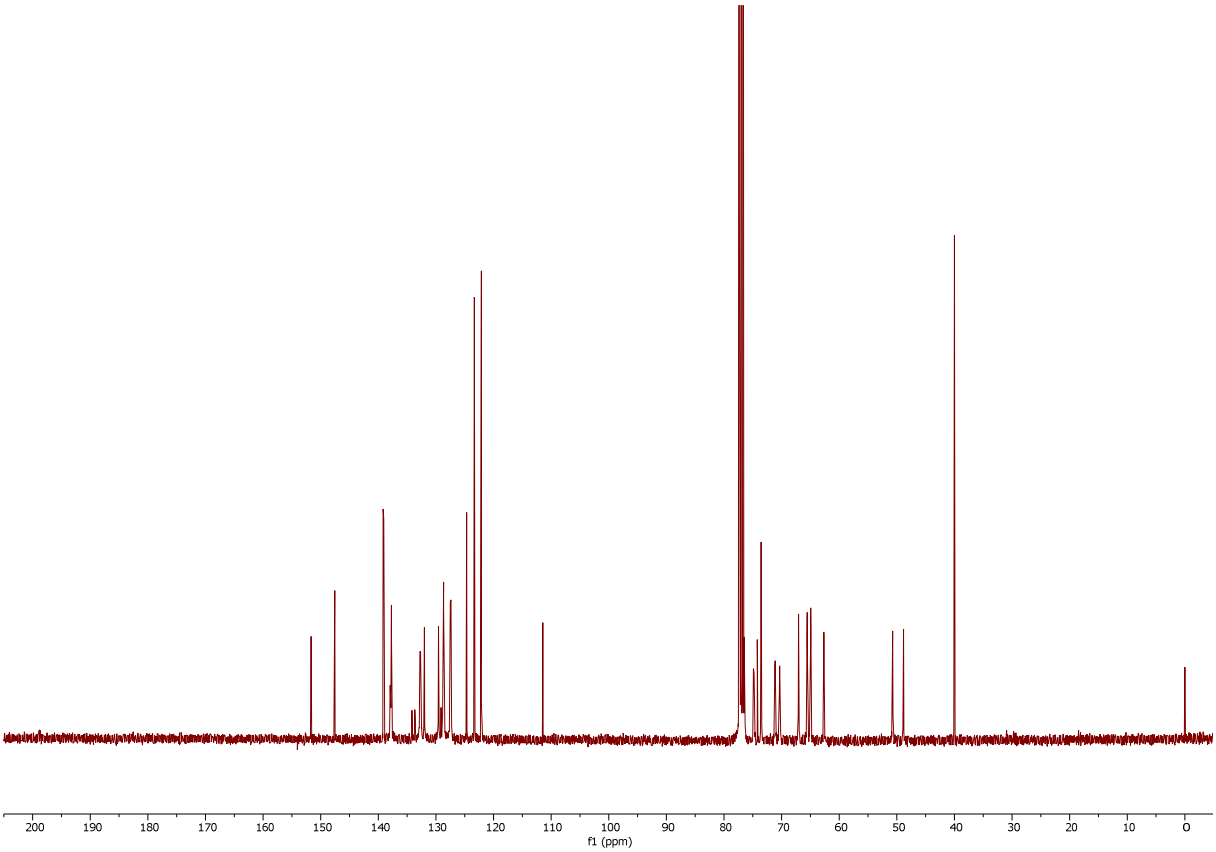


**Figure S27.** $^{13}C\{^{1}H\}$ NMR (101 MHz, $CDCl_3$) spectrum of **7**.

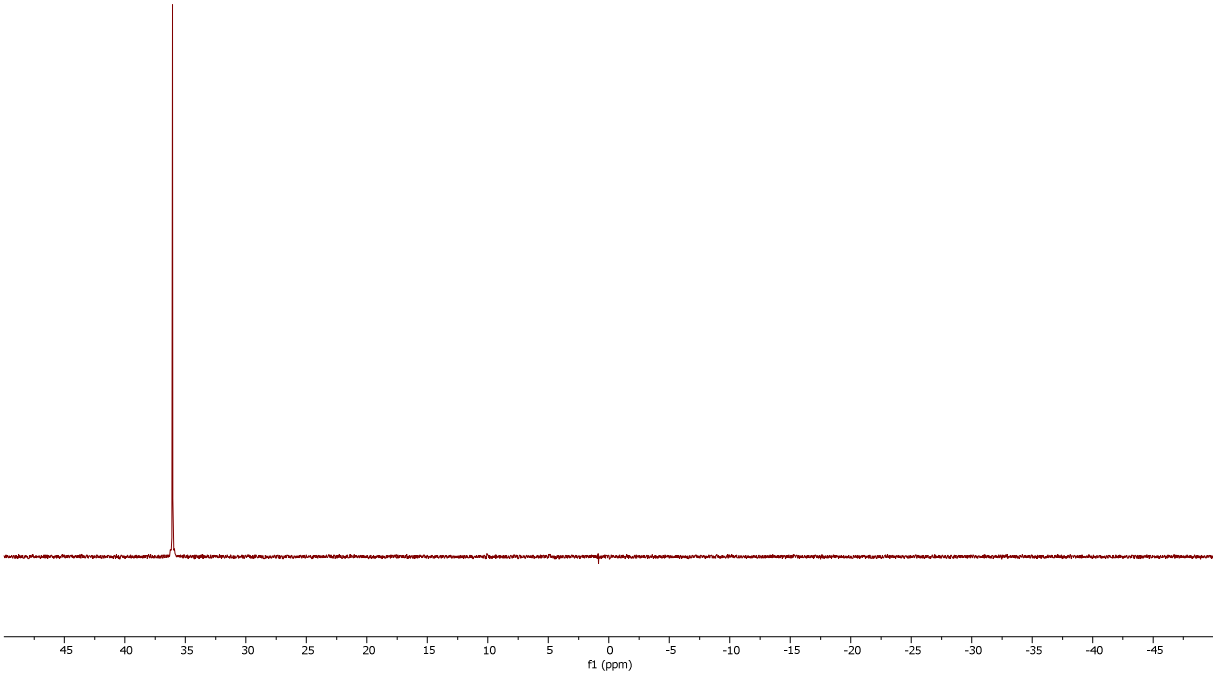


**Figure S28.** $^{31}P\{^{1}H\}$ NMR (162 MHz, $CDCl_3$) spectrum of **7**.